

Investigation of H₂O and OH Masers in the Region of Formation of a Young High-Mass Stellar Object (S255 NIRS 3)

N. T. Ashimbaeva^a, E. E. Lekht^{a,*}, V. V. Krasnov^b, and V. R. Shoutenkov^c

^a*Lomonosov Moscow State University, Sternberg Astronomical Institute, Moscow, 119991 Russia*

^b*Lebedev Physical Institute, Russian Academy of Sciences, Astro Space Center, Moscow, 117997 Russia*

^c*Pushchino Radio Astronomy Observatory, Astro Space Center, Lebedev Physical Institute, Russian Academy of Sciences, Pushchino, 142290 Russia*

**e-mail: lekht@sai.msu.ru*

Received February 14, 2024; revised March 27, 2024; accepted April 23, 2024

Abstract—The results of research of a star formation region S255 IR, where a young high-mass star is forming ($20M_{\odot}$) are presented. Observations in H₂O were carried out with RT-22 in Pushchino, and in the OH lines with the Large Radio Telescope in Nance (France). We used observations in the H₂O line at 1.35 cm for the time interval from 2017 to 2023. Our observations in H₂O showed the presence of strong flares, especially in 2023. A drift of the source emission along the radial velocity was also observed for most spectral features and predominantly with a tendency to decrease the radial velocity. In OH lines at 18 cm in 2008 no emission was detected. We observed OH emission in the main lines at 1665 and 1667 MHz in 2015, 2023, and 2024. Structures of spectra, degrees of circular and linear polarizations varied greatly during these epochs. However, the longitudinal magnetic field vectors had predominantly two directions $\sim\pm(30^{\circ}-40^{\circ})$ relative to the vertical, i.e. almost perpendicular to the jet or along it. Zeeman splitting was detected only in the 1667 MHz line for one pair of features: 2.26 and 2.37 km/s. The splitting value of 0.11 km/s corresponds to a longitudinal magnetic field value of 0.31 mGs; the field is directed towards the observer. It is assumed that the appearance of OH maser emission in 2015 associated with an accretion flares. Significant structure changes of OH spectra, their degrees of polarization and very strong flares of H₂O maser in 2023 may be associated with a new possible accretion flares in S255 IR.

Keywords: star formation, H₂O and OH masers, molecular clouds and bipolar outflows, magnetic field, individual objects (S255 IR)

DOI: 10.1134/S1063772924700434

1. INTRODUCTION

S255 IR is a compact region of active star formation located at a distance of 1.78 kpc from the Sun [1]. Currently, this distance value is considered the most preferable. Eight HH (Herbig-Haro) objects, two large molecular outflows (jets) and numerous sources of infrared emission were observed in this region. The ultra-compact region H II G192.58P 0.04 [2] closest to S255 IR, associated with one of the molecular jets [3], is located north of S255 IR at a distance of 64'' from it.

The 22 GHz H₂O line maser in S255 was discovered by Lo and Burke in 1973 [4]. The maser is located in the S255 IR complex, which lies between the two regions S255 and S257, which turn out to be extended radio sources with a continuous spectrum.

The OH line maser was discovered in 1971 by Turner [5]. Evans et al. [6] measured the position of the source at a frequency of 1665 GHz, but since the

flux was very weak (recorded in only one channel), a comparison with an H₂O maser and the corresponding strong infrared source was made. But since then, no hydroxyl line emission has been observed in this object either at the 18 cm line [7] or at the 5 cm line [8].

In the S255 IR direction there are two Class I and II methanol masers, which were discovered by Haschik et al. [9] and Menten [10], respectively. The fact is that CH₃OH masers of the first type appear in star formation regions. But if Class II methanol masers coincide in location with OH, H₂O masers, and ultra-compact H II regions, then Class I masers are not associated with any known objects, although they are located in the edge region of star formation near the boundaries of dense gas and dust clouds. Class II masers often located in high-velocity matter flows along straight lines or arcs. Norris et al. suggested that they arise in protoplanetary disks [11].

Of great interest are star formation regions in which there are massive young stellar objects with

$M_* > 8M_\odot$, and luminosity $L_* > 5 \times 10^3 L_\odot$. Such objects include the star formation region S255 IR, the mass of the central star in which is about $20M_\odot$ [12]. The interest is due to the fact that in such regions there is a sharp increase in fluxes in the continuum along the wavelength, from radio to infrared emission.

In the last few years, bright flares of accretion have been discovered in such massive young stellar objects as, for example, S255 IR, NGC 6334 I, G358.931–0.030, and G24.33+0.14 [2]. It was these events that were accompanied by flares of maser emission, as well as flares of radio emission—in the millimeter and sub-millimeter wavelength ranges. For example, in the direction of a massive young stellar object in S255 IR, a significant flare was observed in the methanol maser line at 6.7 GHz in November 2015 [13], which is explained by an increase in accretion luminosity in mid-June 2015 [12].

Extended H₂O maser emission (>1700 AU) was first detected in S255 IR [14]. Moreover, maser emission from both compact and extended regions has the same flux changes with time. The authors believe that these regions have a common excitation mechanism – radiative excitation due to the combined effect of an IR flash and an expanding jet. Monitoring of the H₂O maser, carried out from 1981 to 2000, showed that the variability of the integral flux has a cyclic pattern [15].

This paper is devoted to the study of flares during the time interval from 2017 to 2023. The full catalog of spectra and the results of their analysis will be published in our subsequent paper on S255 IR. Time interval from 2017 to 2023 was chosen in this work for two reasons. First, our research is to some extent an answer to questions posed by Hirota et al. [14] (for example, about the reason for the absence of a sudden and strong increase in the intensity of the H₂O maser after the accretion flare in 2015). Secondly, during this interval there was a significant increase in the integral flux and the strongest flares of water vapor maser emission occurred over the entire time interval of our monitoring of this source. We do not present here the monitoring data for 2015–2016, since the spectra for this interval were published by Hirota et al. [14]. All spectra will be presented in the announced paper.

2. EQUIPMENT AND OBSERVATIONS

We observed the H₂O maser source in S255 IR in the 1.35 cm line by the 22-m radio telescope of the Pushchino Radioastronomy Observatory (PRAO) since the end of 1981. Source coordinates: $\alpha_{(2000)} = 6^{\text{h}}12^{\text{m}}54^{\text{s}}$ and $\delta_{(2000)} = +1^\circ 59' 23''$. Results of observations from 1981 to 2000 were published in the work of Pashchenko et al. [12].

The width of the beam pattern of the radio telescope at a wave of 1.35 cm is 2.6'. The noise temperature of the system was in the range of 150–300 K, depending on the observation conditions. The sensitivity of the telescope is 25 Jy/K.

The signal was recorded by a 2048-channel auto-correlation receiver with a radial velocity resolution of 0.0822 km/s. The accuracy of radial velocity determination was within 20–25 m/s. The intervals between observation sessions were generally about one month. However, when strong flares occurred, we made several observations within one session (3–4 days).

We also carried out polarization measurements of the OH maser emission characteristics in S255 IR at 18 cm by the Nance radio telescope (France) in 2008, 2015, 2023, and 2024. The sensitivity of the telescope is 1.4 K/Jy. Observations were made in the main lines at 1665 and 1667 MHz. Spectral resolution during 2008 and 2015 in the 1665 MHz line was 0.1373 km/s, and in 2023 it was 0.0687 km/s. Six radiation modes were obtained: two modes in circular polarizations (left and right) and four modes in linear polarization for the antenna feeder directions 0°, 45°, 90°, and 135°. The observation methodology and data processing were repeatedly described in feature in our previous publications (see, for example, [13, 14]).

3. OBSERVATION RESULTS

Figures 1–7 show the central parts of the spectra where H₂O maser emission was observed. The spectra are shown for the 2017–2023 interval. For each spectrum, the observation epoch is given. All spectra are corrected for absorption of emission in the Earth atmosphere. This was included in the observation program. As noted earlier, we are preparing to publish a complete catalog of H₂O spectra in S255 since our monitoring of this source in 1981, including a 3D representation of all spectra. This is very important for illustrating the flare nature of H₂O maser emission and studying the evolution and patterns of flare occurrence.

In Figure 8, we show the variability of the integral flux calculated in the range of radial velocities from –15 to +20 km/s. A quasi-periodic nature of variability is observed. The constant component of the integral flux, which is reflected by a straight line, and activity cycles are highlighted. For most of them, the radial velocities of the most intense features are indicated in the flux maxima.

In each H₂O spectrum, individual emission features were identified and their flux densities and radial velocities were determined. The variability of the radial velocity of the main features is shown in Fig. 9. Large light circles mark features in those epochs when their flux density exceeded 200 Jy. The velocity variations of the most intense features are approximated by straight line segments and these features are numbered

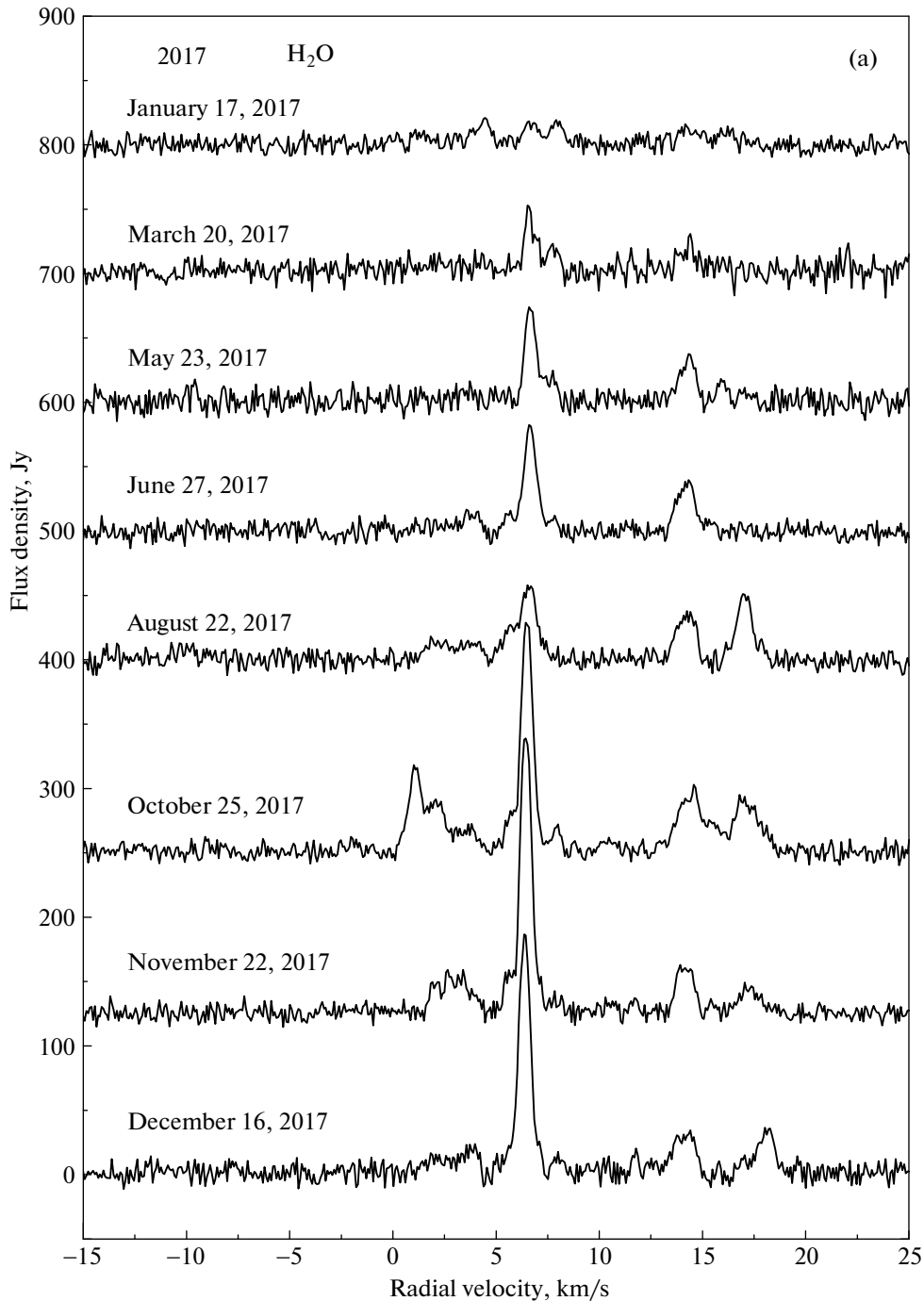


Fig. 1. Spectra of H₂O maser emission in the direction of S255 IR, obtained in 2017. Observational epochs are indicated.

from 1 to 12. The slopes of the straight lines reflect the tendency of features to drift in the spectrum. Of course, the real drift has a more complex character with respect to inscribed straight lines, for example, for features 1, 4, and 9. On the left part of the plot, asterisks show the positions of the H₂O features for the epoch of May 14, 2017, taken from ([11], Table 4). Shaded asterisks indicate masers observed at 22 GHz, and open asterisks mark masers observed at 321 GHz.

Hydroxyl line emission in S255 IR was not observed in 2008, with an upper limit of about 0.1 Jy. Results of OH observations in 2015, 2023, and 2024 in the main lines at 1665 and 1667 MHz are shown in Figs. 10–12 and 13–15, respectively. The upper panels (a) show spectra in circular polarizations. Panels (b) show the Stokes parameter V , defined as the difference in emission in the right and left circular polarizations. When registering linear polarization, a signal is first

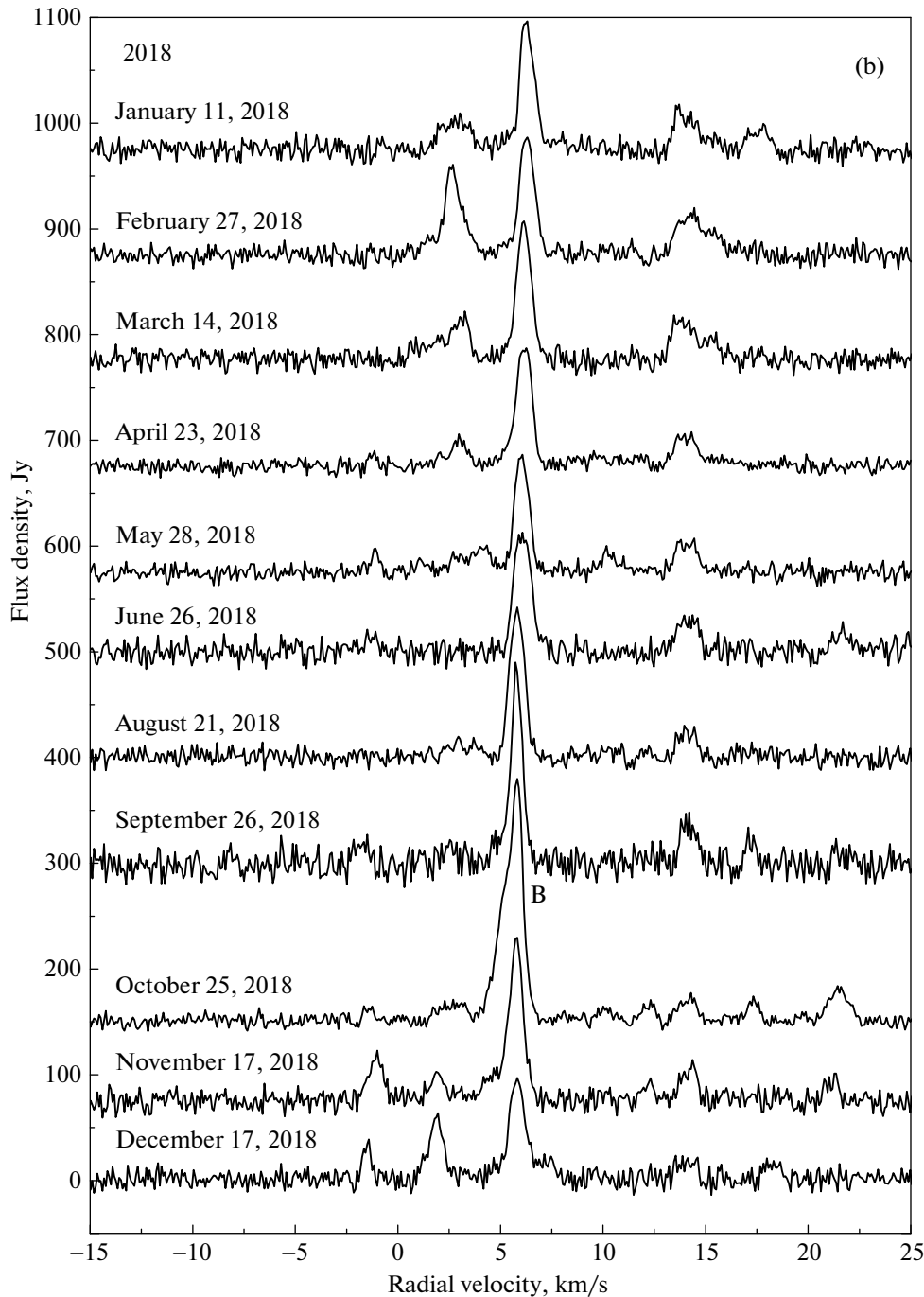


Fig. 2. Continued. Same as in Fig. 1, for 2018.

received from two orthogonal directions 0° and 90° (panel c), and then after rotating the antenna feeder by 45° from the direction 45° and 135° (panel d).

4. DISCUSSION

4.1. Maser Emission from Water Vapor

The identified features in the H_2O spectra showed that the features (more precisely, maser condensations responsible for the emission) exist for a long time, but

their activity changes significantly and, often, over a wide range of intensities.

A large number of flares of different intensity and duration were observed during the monitoring interval from 2017 to 2023. The increase in maser flux may be directly caused by collisions in the jet, which is ejected from the star and emits in the radio continuum. According to Hirota et al. [11], it is possible that the change in water maser emission observed in their monitoring is not at all related to the accretion flare,

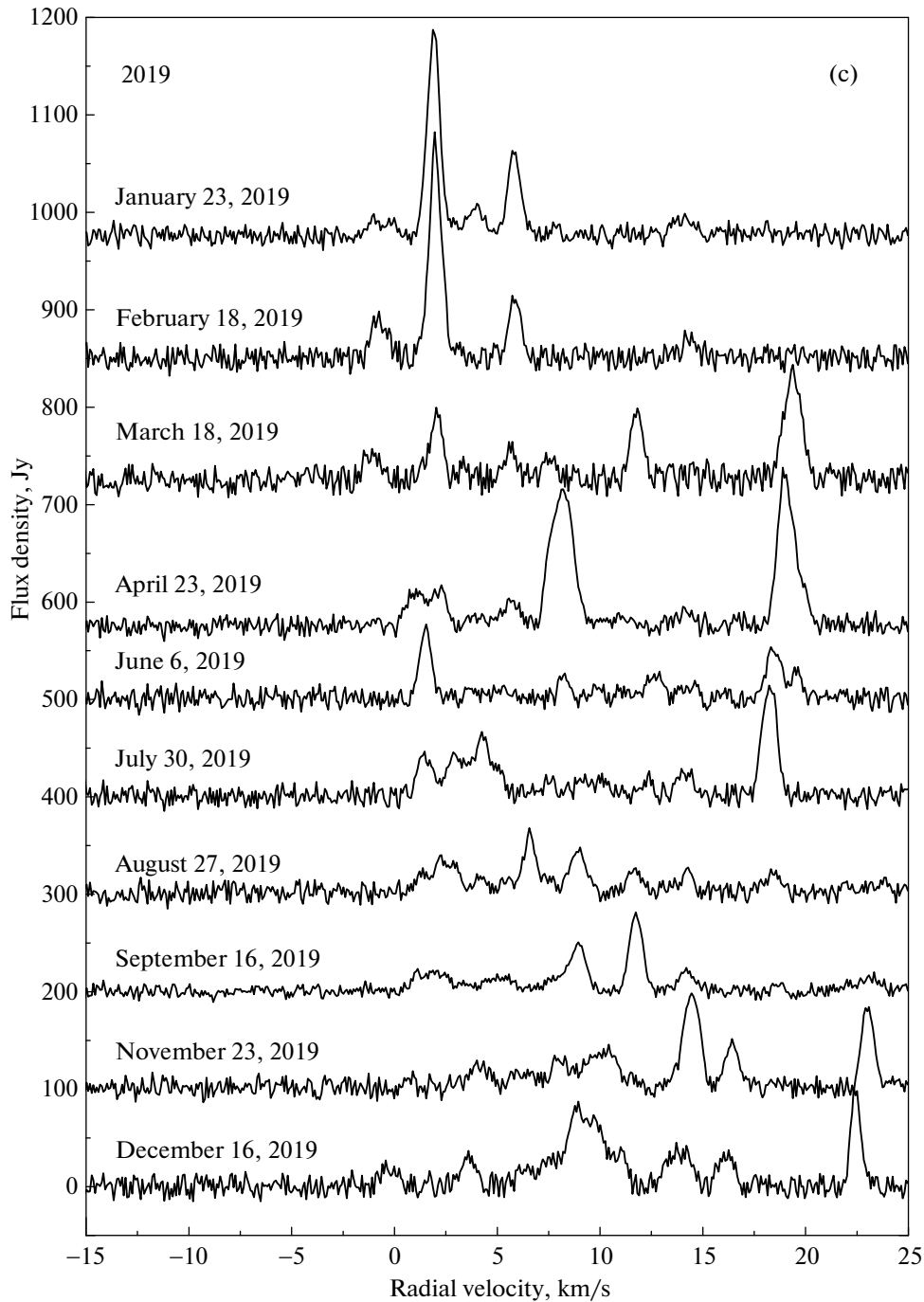


Fig. 3. Continued. Same as in Fig. 1, for 2019.

the consequences of which have been observed in other indicators.

Despite frequent flares occurring at different radial velocities, some periodicity is still visible in the variability of the integral flux. Most likely, we can talk about alternating maxima and minima of maser activity, which is associated with non-stationary processes of the formation of a central high-mass star in S255 IR.

Most features have radial velocity drift. The drift with a tendency to decrease radial velocity predominates significantly. The cause of the drift may be the intrinsic motion of maser condensations in the jet, and the influence of turbulent motions of matter is also possible.

The main emission feature, according to Hirota et al. [11], had a radial velocity 6.4 km/s, which decreased with time. The observed increase in the flux

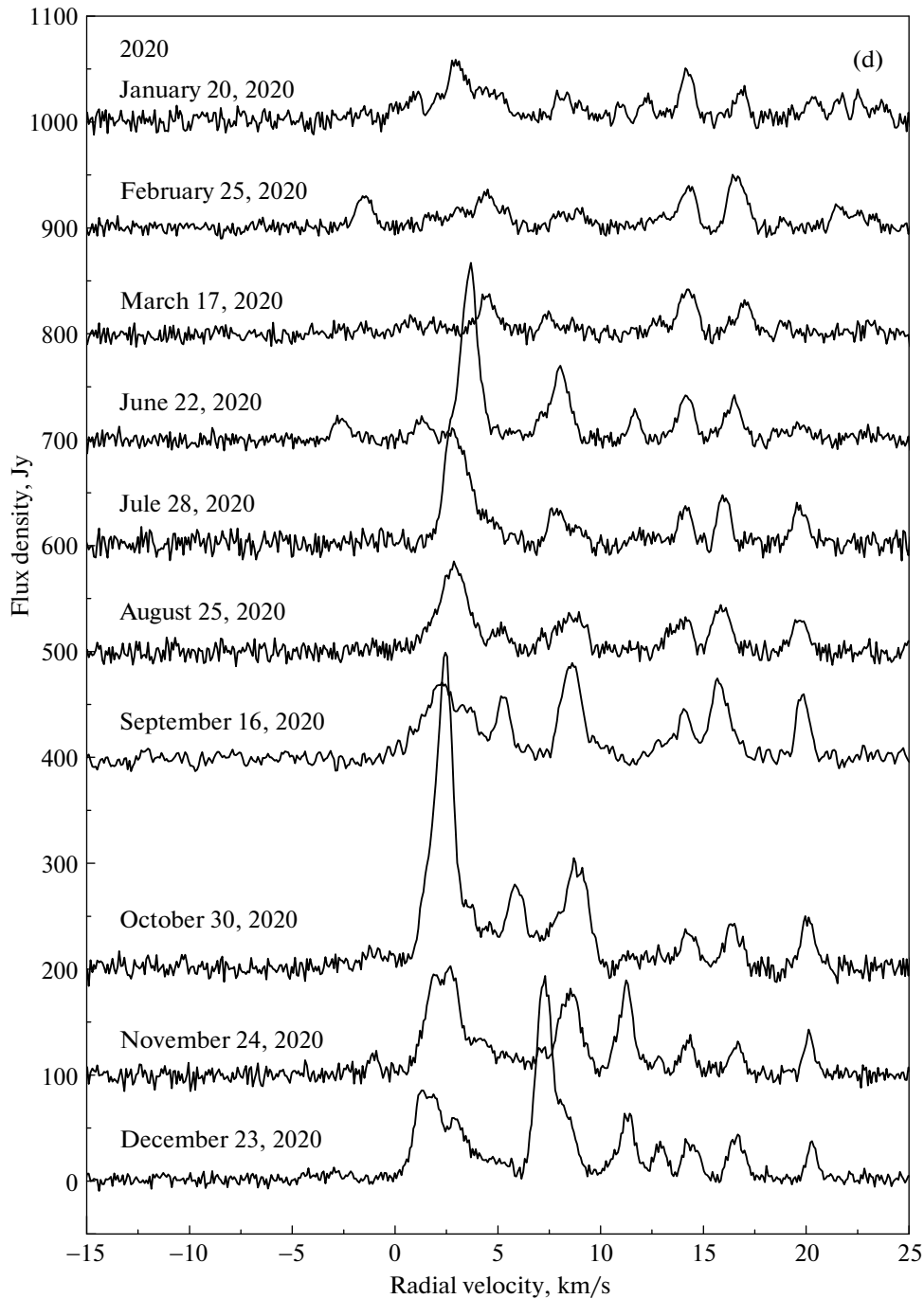


Fig. 4. Continued. Same as in Fig. 1, for 2020.

of this feature in 2017–2018, according to the authors, may be caused by the expanding jet in which this feature is located. Our monitoring shows that from the second half of 2017 to the end of 2018, the flux did more or less remain at the same level (see Fig. 16), but there were two relatively small flares. In December 2017, the flux density at the maximum of the first flare was 210 Jy, and in October 2018 for the second flare it was slightly higher, 230 Jy. After this flare, a rapid

decline in flux began and, especially, in 2019, when a significant drop in emission to the minimum detectable value ($\sim 5\text{--}10$ Jy) and a further decrease in radial velocity took place (see Figs. 3 and 4). From June 2019 to October 2022, emission from this feature appeared only sporadically.

But later in the region of this radial velocity the spectrum was quite complex. Since the beginning of

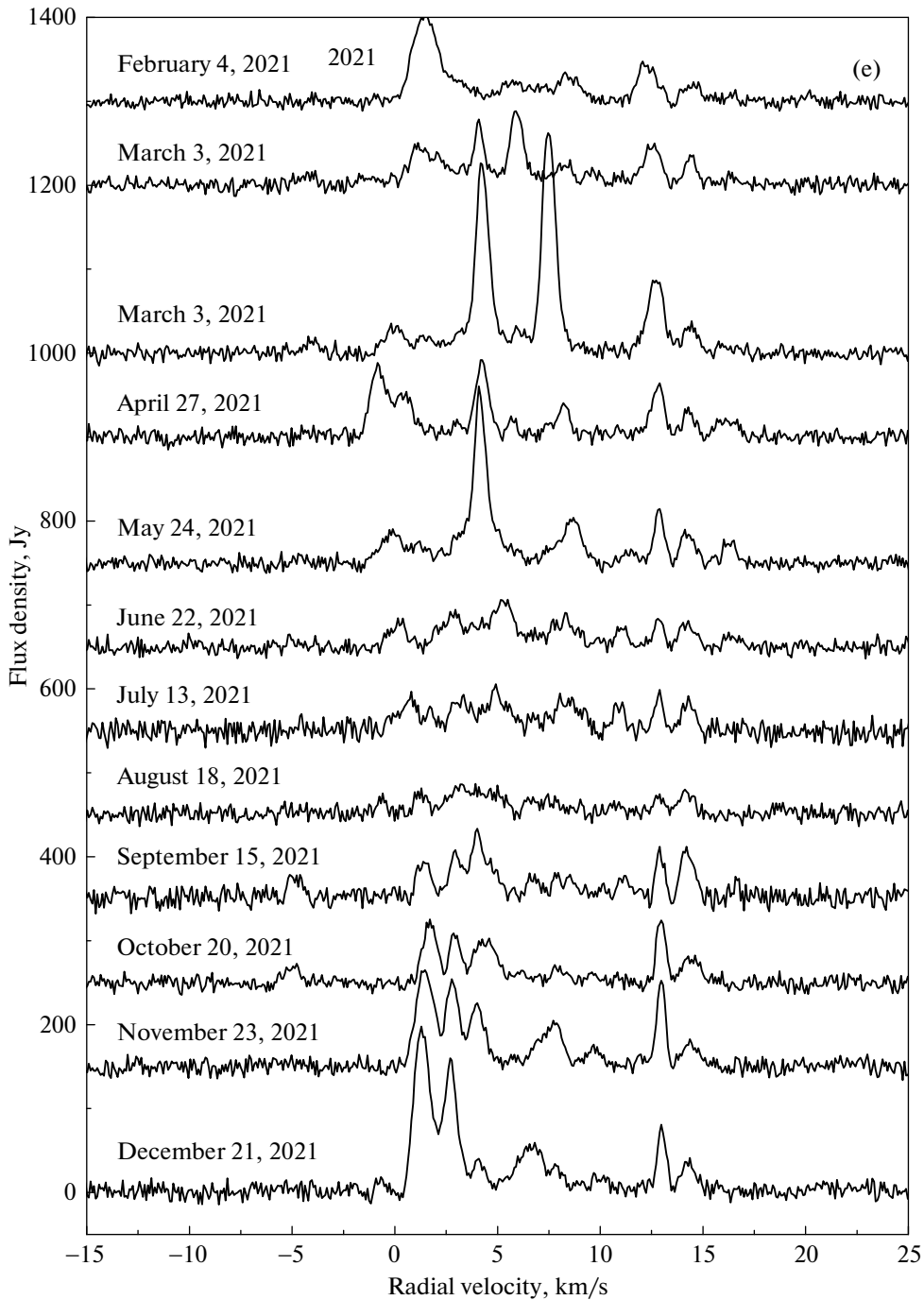


Fig. 5. Continued. Same as in Fig. 1, for 2021.

2023, a series of three consecutive strong flares have been observed (see Figs. 7 and 16). The first had a velocity of 4.76 km/s and a flux density of 510 Jy. The second short-term flare occurred at a velocity of 4.3 km/s with a maximum flux density of about 1000 Jy. The third flare had a velocity of 4.6 km/s, the maximum flux density reached 3100 Jy and the flare had a longer duration than the second flare.

4.2. Hydroxyl Maser Emission

Four epochs of observations do not allow us to accurately estimate the onset of the hydroxyl maser flare. It is important that all cataclysms in the source began to occur in 2015. It can be assumed that this also applies to the hydroxyl maser. The main result of our OH observations is the existence of strong emission variability in both main lines: 1665 and 1667 MHz.

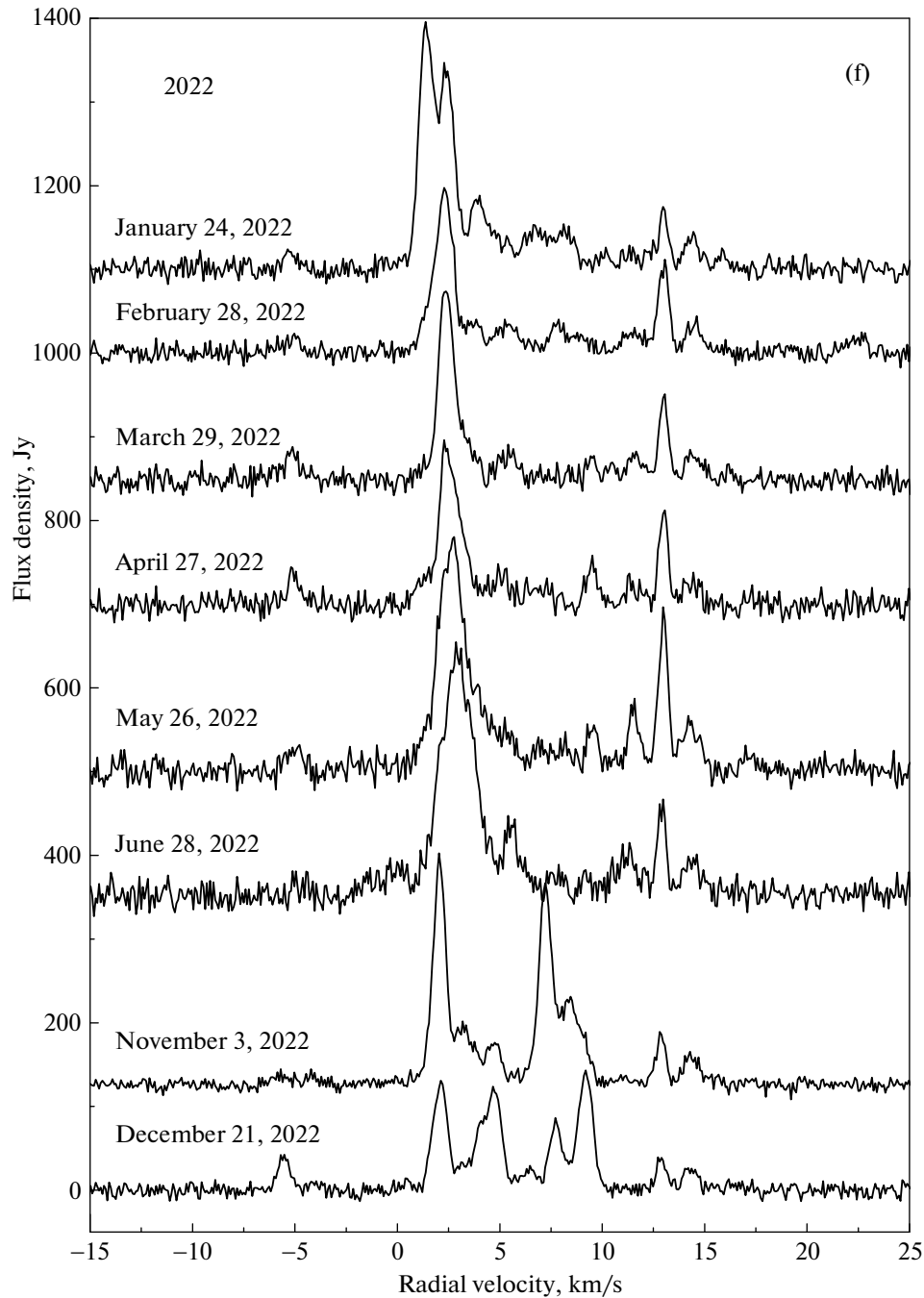


Fig. 6. Continued. Same as in Fig. 1, for 2022.

If we consider the picture of polarization variability for the source on a global scale (Figs. 10–12), then we can argue that in the 1665 MHz line in 2015 spectra were quite simple (Fig. 10). Strong circular polarization was present and very weak linear polarization was also present. We can assume that there was a significant depolarization of the OH maser emission, as occurs in the W51 Main source [18]. In 2023, the spectra changed significantly (Fig. 11). They became more complex and included a large number of emission fea-

tures. The degree of circular polarization decreased significantly, and the degree of linear polarization increased significantly and in some features it reached about 40–60%. In 2024, strong changes occurred in the polarization parameters of individual features (Fig. 12).

A different evolution pattern was observed in the 1667 MHz line (Figs. 13–15). The spectra in 2023 became simpler than in 2015, i.e., the number of fea-

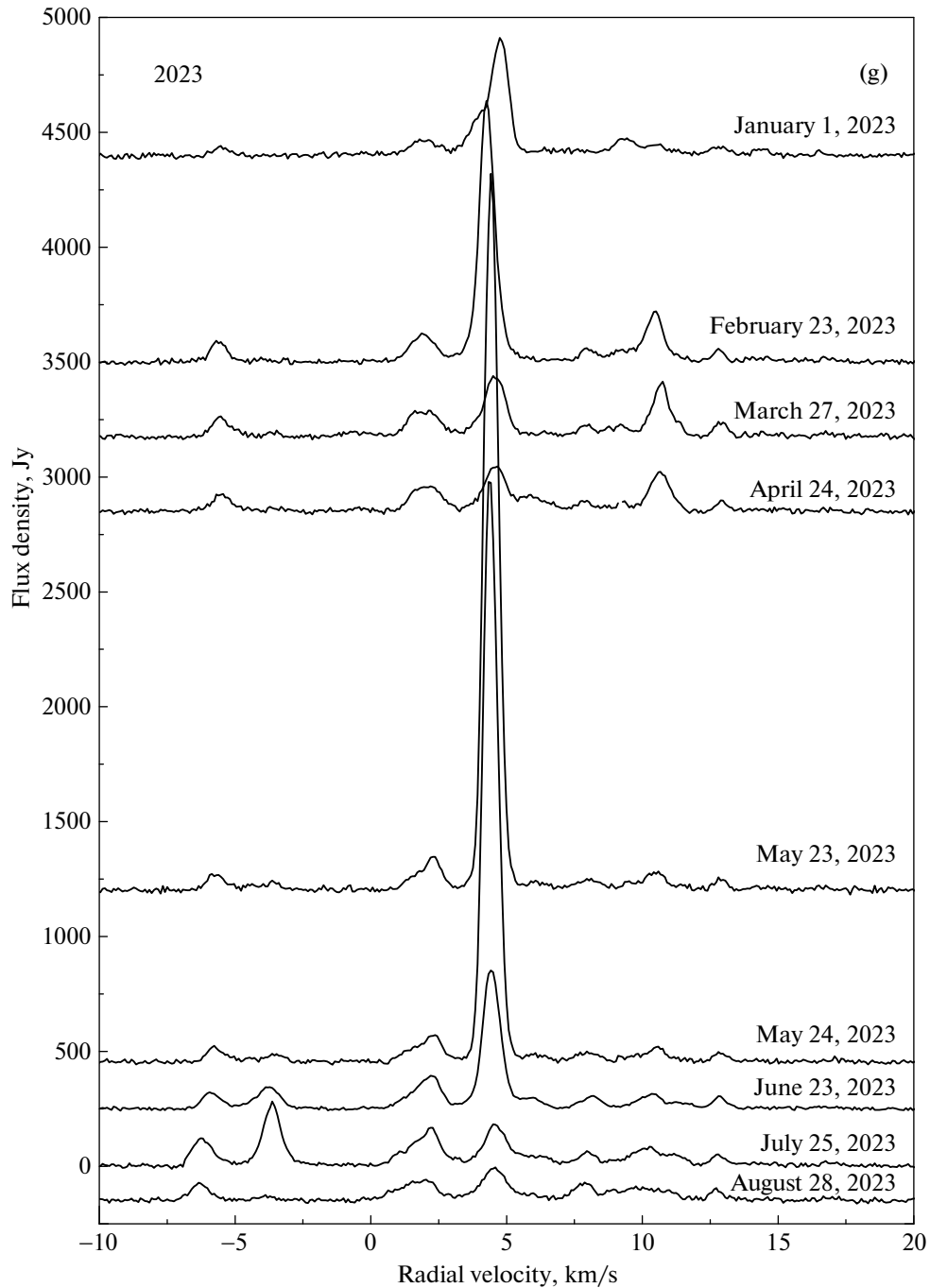


Fig. 7. Final spectra. Same as in Fig. 1, for 2023.

tures in the active stage of emission decreased. The degree of circular and linear polarization has decreased.

Thus, to the available information on accretion outbursts, we can add that during the accretion flare in S255 IR in 2015, there was also a flare of OH maser emission in both main lines.

Panels (a), (b), and (c) of Figure 17 show the degrees of circular (m_c) and linear (m_l) polarizations

and the positional angle (χ) of linear polarization of individual features in the OH 1665 and 1667 MHz lines at different observation epochs. For ease of perception of the plot and its analysis, we took into account that, for example, an angle -60° is the same angle as 120° . That's why we made these replacements. The points on the plots are not randomly located, but there is some relationship between the polarization parameters and the radial velocity.

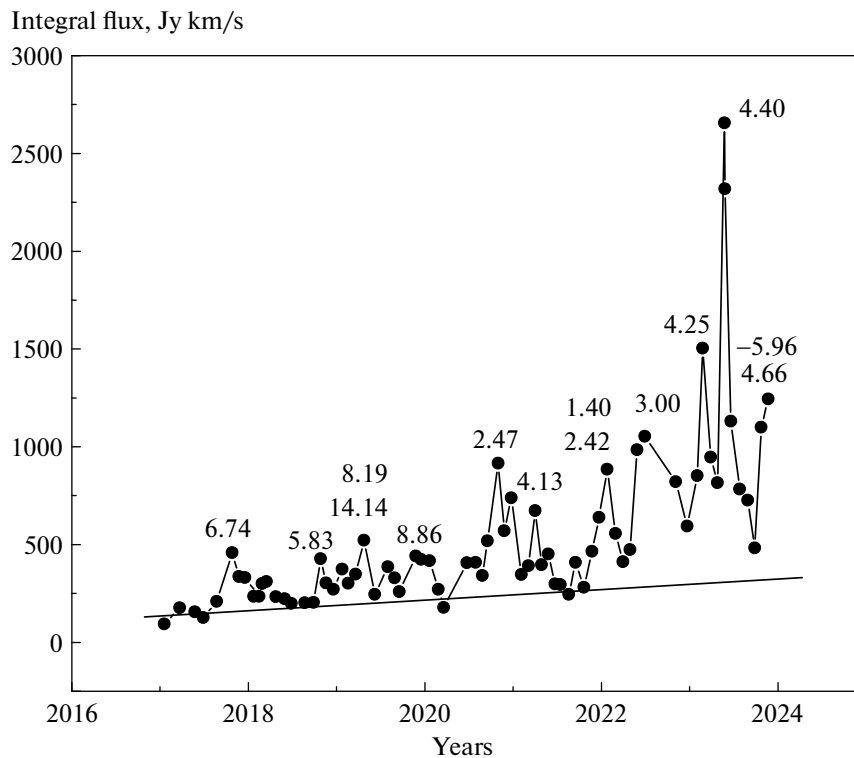


Fig. 8. Variability of the integral flux of H₂O maser radiation in the S255 IR direction. For each maximum, the radial velocities of the most intense features are indicated.

Panels (d) of Figure 17 straight line segments show the transverse magnetic field vectors for individual maser features at different observation epochs. There are two preferential directions of the transverse magnetic field $\sim\pm 30^\circ$ relative to the vertical. In the 1665 MHz line in 2023, one direction of the magnetic field predominated $\sim +30^\circ$, and in 2024 both directions were more or less equivalent. Despite the preservation of the structure of the spectrum in the 1665 MHz line, in some features, in a short time (no more than three months), significant changes in the direction of the transverse magnetic field vector occurred at an angle of about 60° – 70° .

Zeeman splitting was detected only in the 1667 MHz line for one pair of features at 2.26 and 2.37 km/s. The splitting value was 0.11 km/s. It corresponds to a longitudinal magnetic field value of +0.31 mG. The field is directed towards the observer. Analysis of other features of the 1665 and 1667 MHz spectra did not reveal the existence of other Zeeman pairs.

For the two main features in the 1665 MHz line, at their average radial velocities of 4.95 and 5.0 km/s, there is a dependence of the radial velocity on the position angle of the antenna (Fig. 18). The change in the velocity of the features occurred in antiphase. The smallest distance between features was observed at the

antenna position angle $\chi = 75^\circ$. This picture was observed for two epochs of 2023 and 2024, which cannot be an accident. We draw attention to the fact that in circular polarizations the complex structure of each of these spectral features is revealed. Thus, we can assume that the observed phenomenon is associated with an inhomogeneous structure of maser condensations, or with a compact accumulation of condensations with fairly close radial velocities. For this reason, the observed shift of the spectral maxima between circular polarizations is not a consequence of Zeeman line splitting.

Flares of OH maser emission and significant changes in the spectral structure in 2023 and 2024, as well as a series of H₂O flares in 2023, may be associated with another recurrent accretion flare in S255 IR.

5. MAIN RESULTS

Let us list the main results obtained in this paper from monitoring the H₂O maser at the 1.35 cm line in Pushchino (Russia) and from polarization observations in the lines of the OH molecule at a wavelength of 18 cm in Nance (France), the region of active star formation S255 IR, in which the young high-mass star (S255 NIRS 3).

—Monitoring in the 2017–2023 interval showed that H₂O maser emission has a flare character.

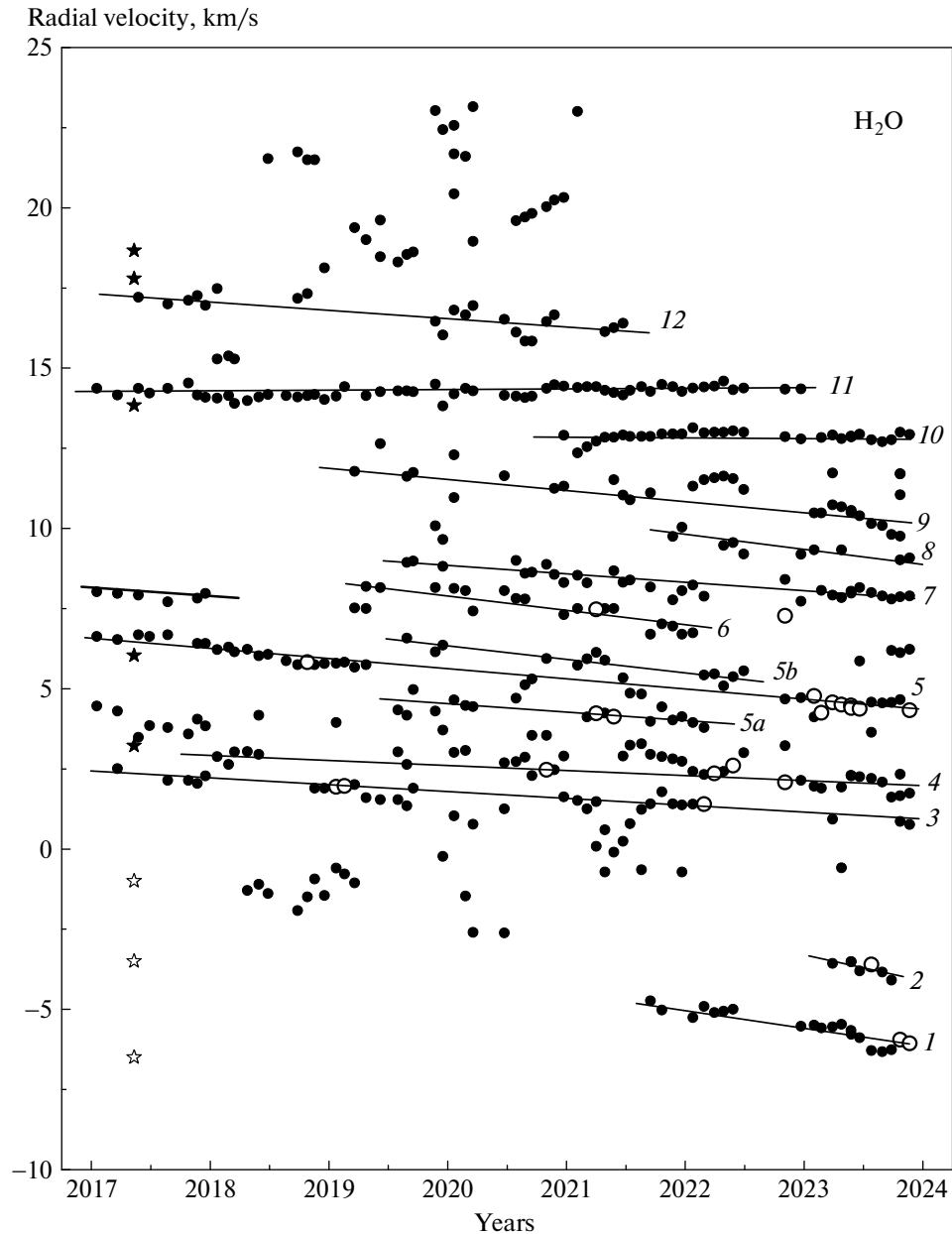


Fig. 9. Variability of the radial velocity of individual emission features in the spectra of H₂O. Large open circles mark features in those epochs when their flux density exceeded 200 Jy. The velocity variability of the most intense features is approximated by straight line segments and these features are numbered from 1 to 12. On the left, asterisks show the positions of the H₂O features for the epoch of May 14, 2017, taken from [11, Table 4]. Shaded asterisks indicate masers observed at 22 GHz, and open asterisks at 321 GHz.

—The integral flux of H₂O changes cyclically with a period of approximately one year.

—Drift is observed in most features and, as a rule, with a tendency to decrease radial velocity.

—No emission was detected in the OH 18 cm lines in 2008. OH emission was observed in the main lines at 1665 and 1667 MHz in 2015, 2023, and 2024.

—The structures of the spectra and the degrees of circular and linear polarization varied greatly during

these epochs. However, in this case, the transverse magnetic field vectors had predominantly two directions $\sim\pm(30^\circ-40^\circ)$ relative to the vertical, i.e., almost perpendicular to the jet or along it.

—Zeeman splitting was detected only in the 1667 MHz line for one pair of features at 2.26 and 2.37 km/s (splitting 0.11 km/s). The magnitude of the longitudinal magnetic field is 0.31 mG and the field is directed towards the observer.

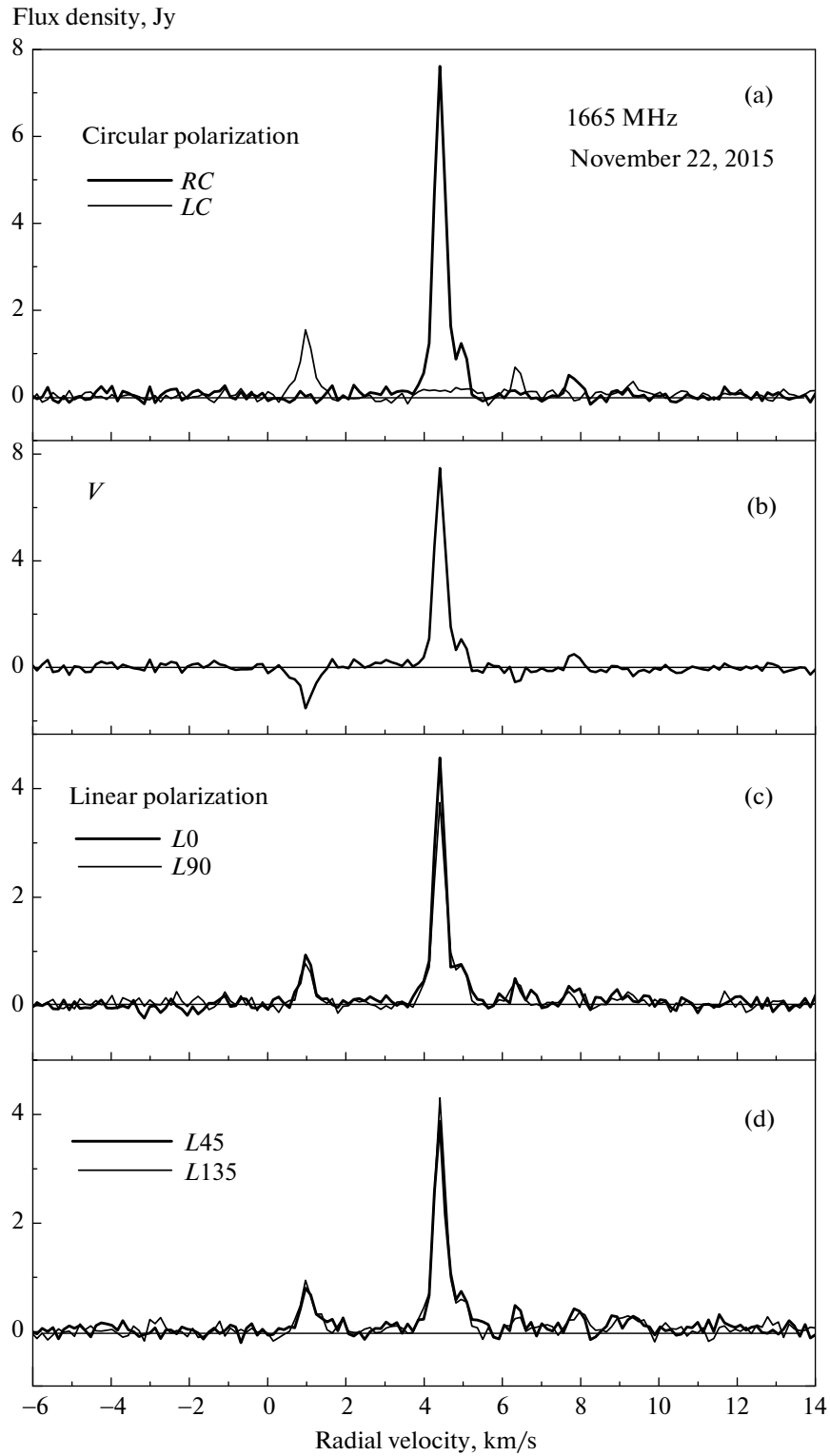


Fig. 10. Spectra of OH maser emission in the main 1665 MHz line in the direction of S255 IR at the epoch of November 22, 2015. The upper panel (a) shows the spectra in the right (thick line) and left (thin line) circular polarizations. Panel (b) gives the Stokes parameter V . The remaining panels show spectra in linear polarization at the antenna polarization plane (PA) positions 0° , 45° , 90° , and 135° .

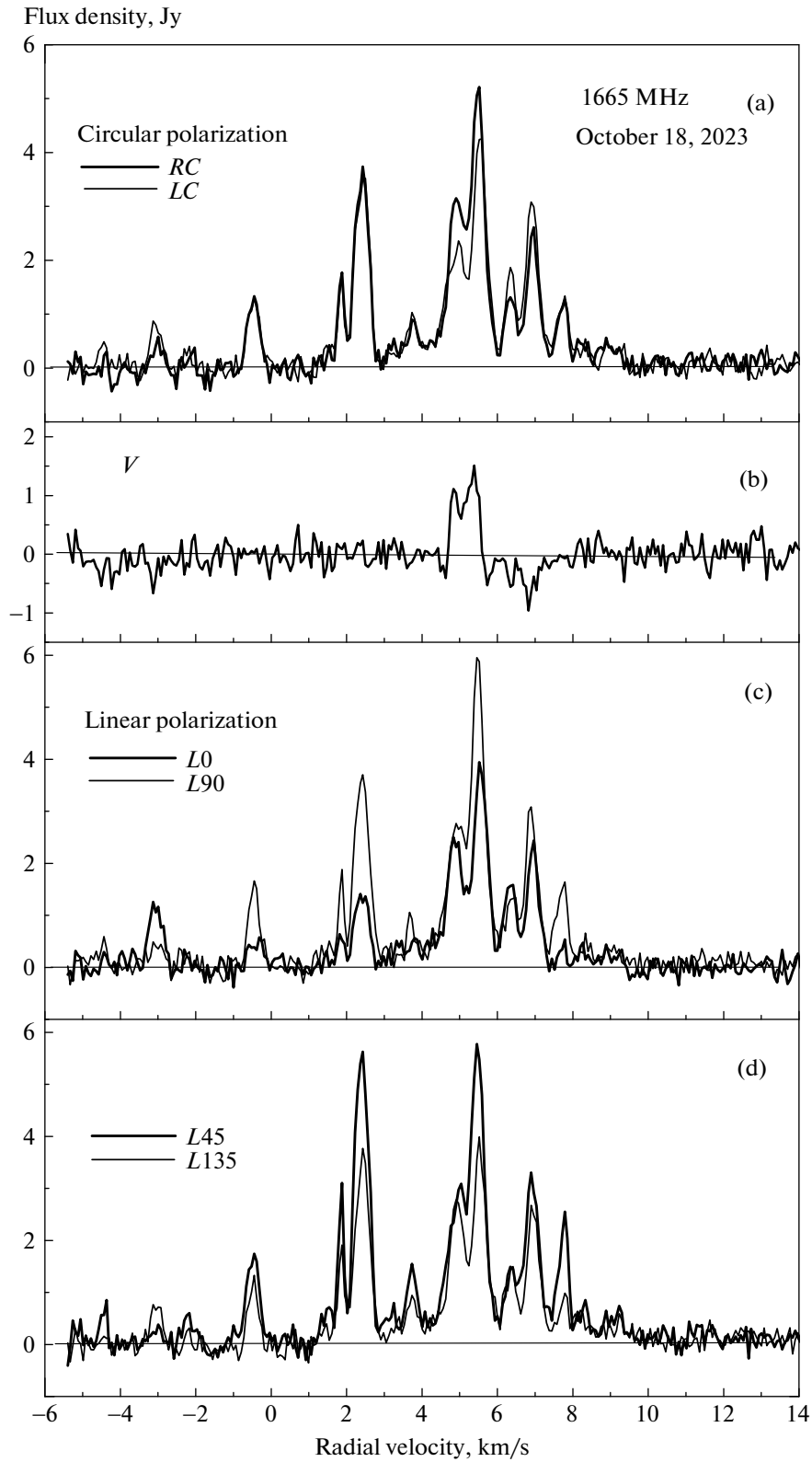


Fig. 11. Same as in Fig. 10, but in the October 18, 2023 epoch.

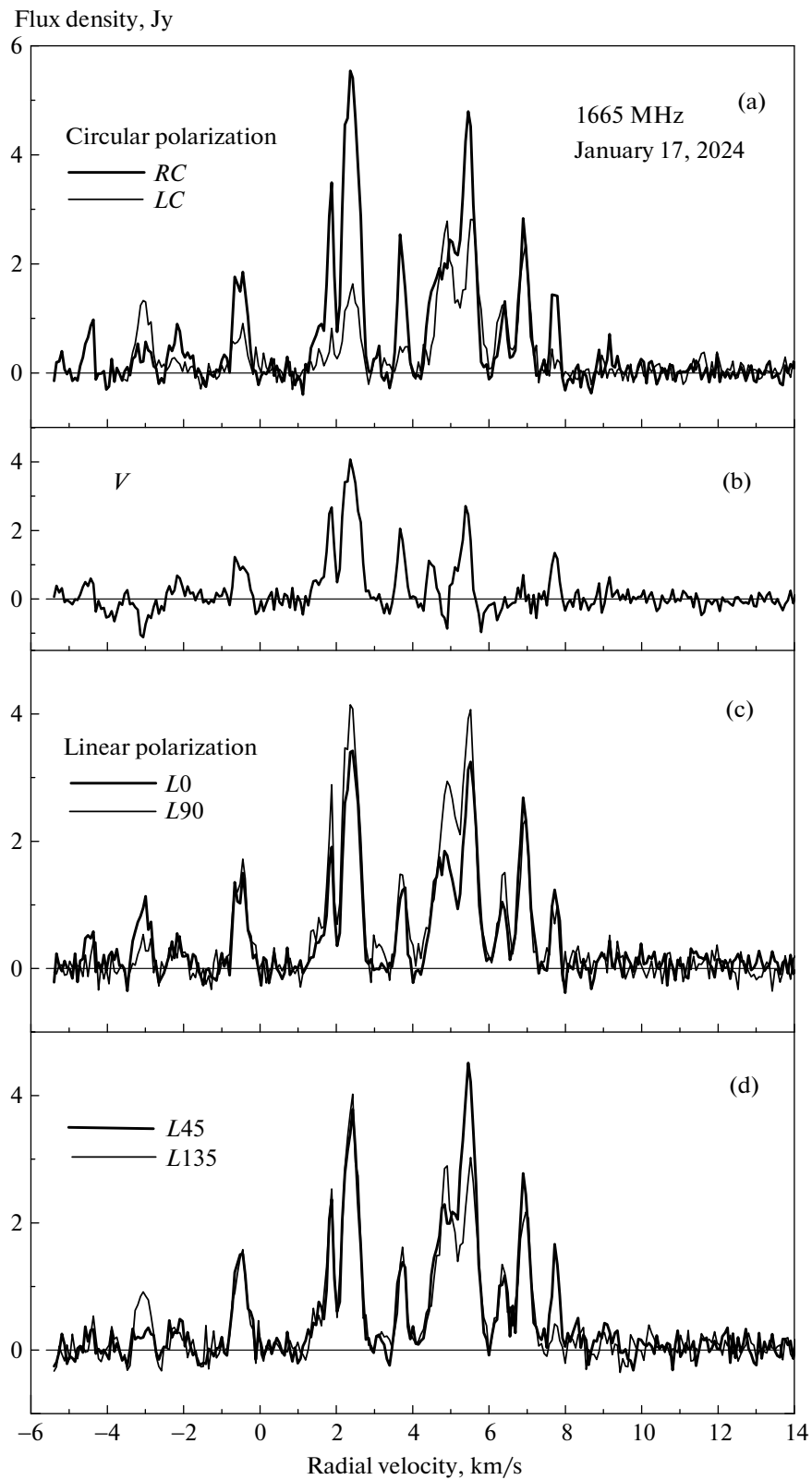


Fig. 12. Same as in Fig. 10, but in the January 17, 2024 epoch.

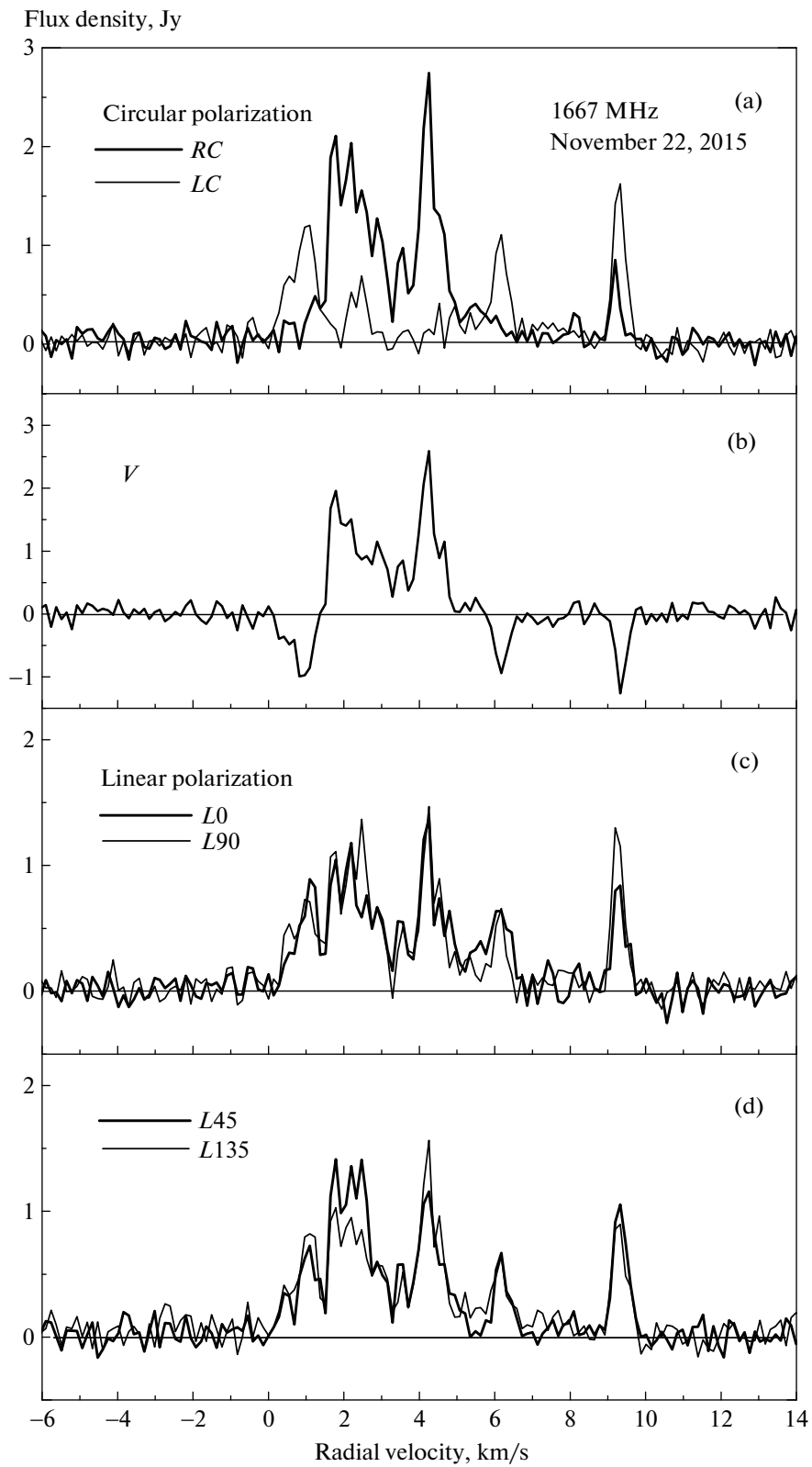


Fig. 13. Same as in Fig. 10, but for the 1667 MHz line in the November 20, 2015 epoch.

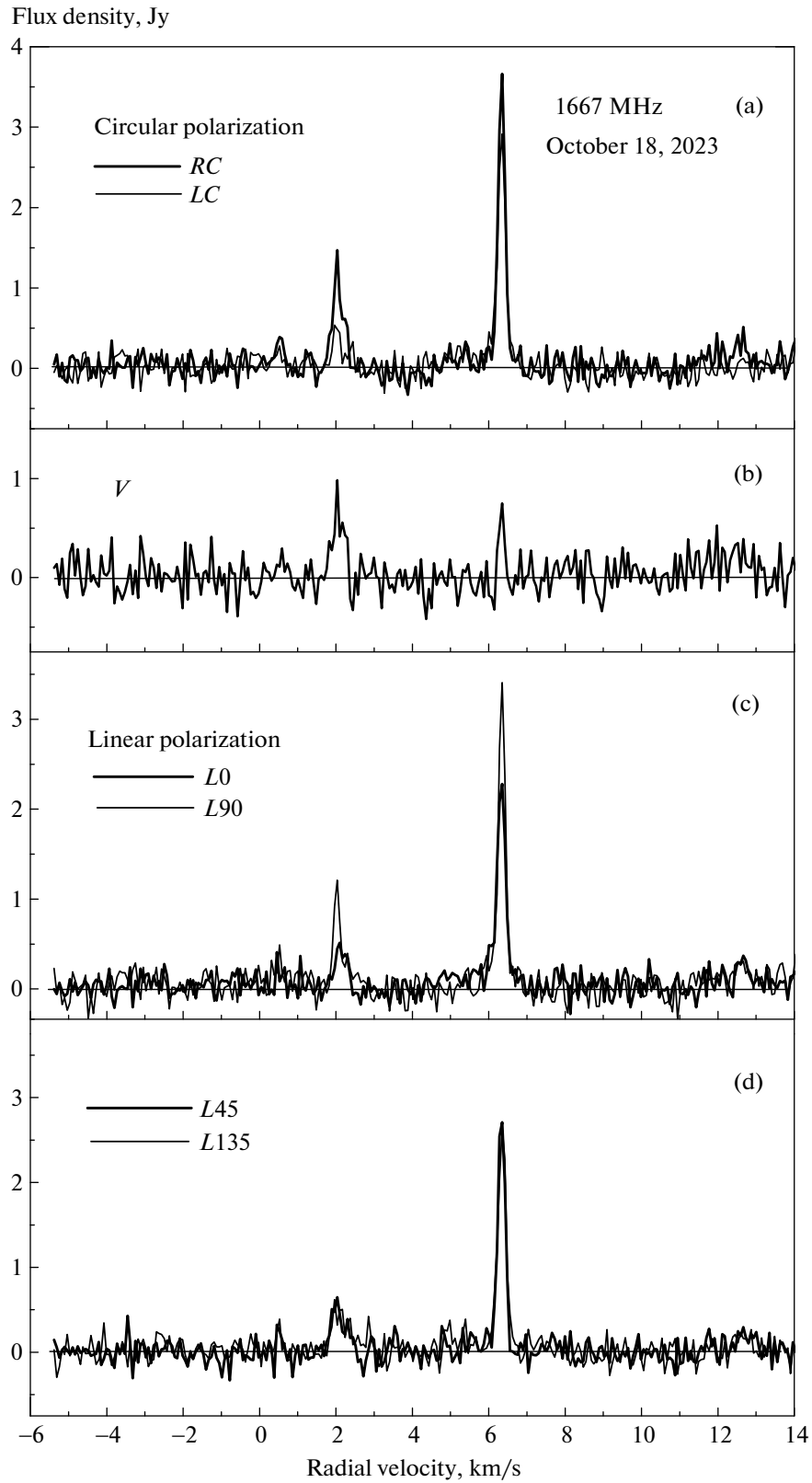


Fig. 14. Same as in Fig. 10, but for the 1667 MHz line in the October 18, 2023 epoch.

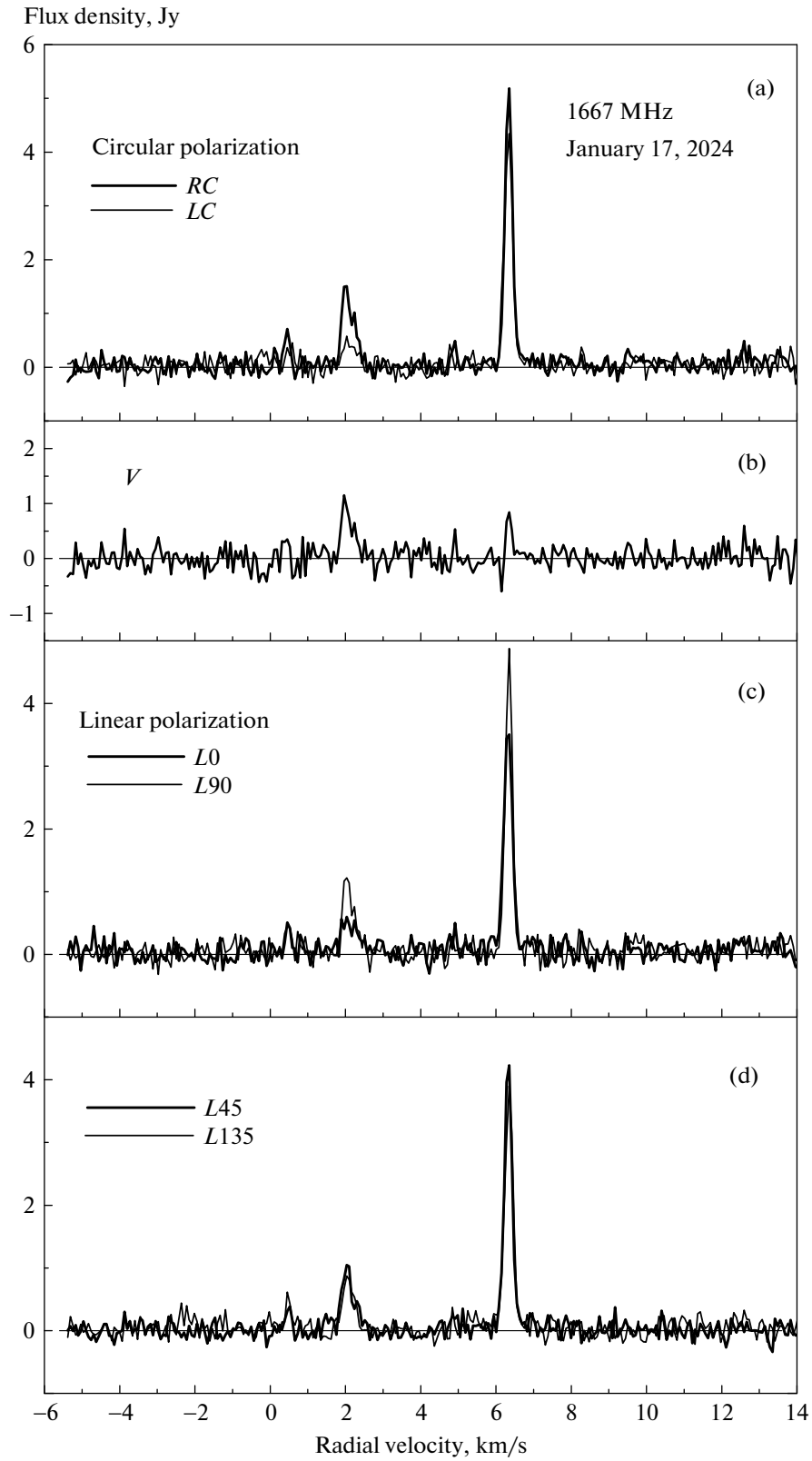


Fig. 15. Same as in Fig. 10, but for the 1667 MHz line in the January 17, 2024 epoch.

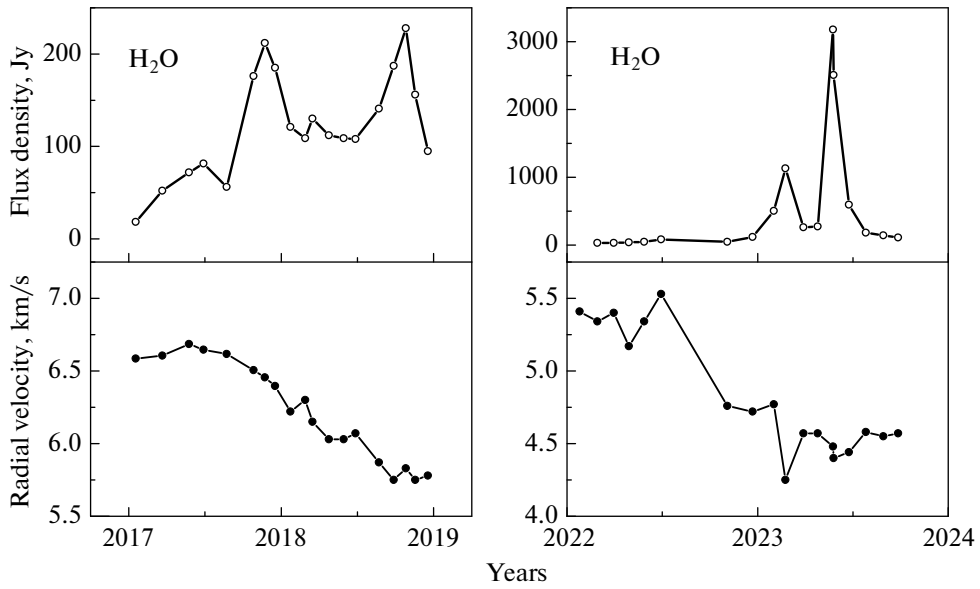


Fig. 16. Variability of flux density and radial velocity of the main feature of the H_2O maser.

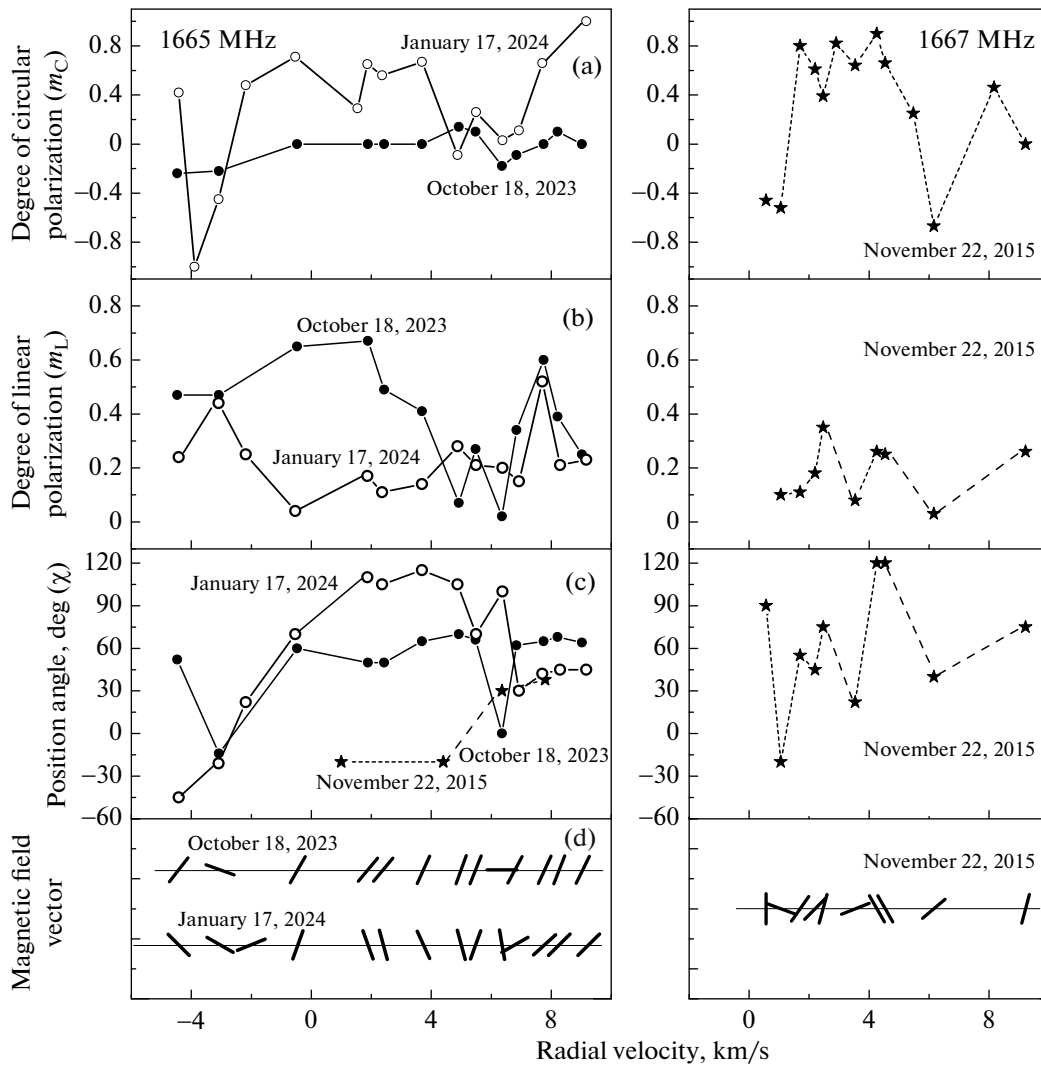


Fig. 17. Plots of the degree of circular (a) and linear (b) polarization, position angle (c) of linear polarization of individual features in the OH 1665 and 1667 MHz lines, as well as the direction of the transverse magnetic field vectors for individual maser features at different observation epochs (d).

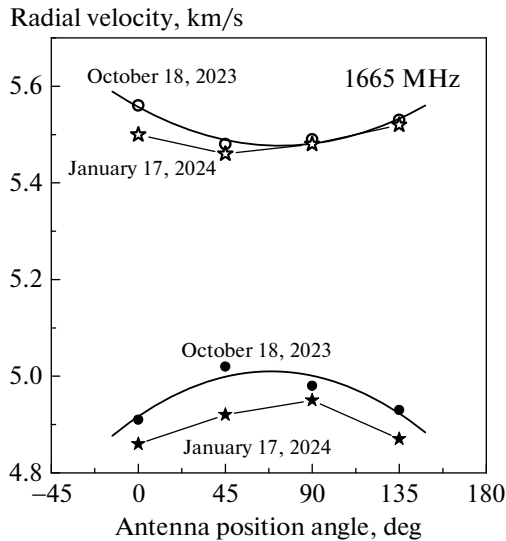


Fig. 18. Dependence of the radial velocity of two features in the 1665 MHz OH line on the position angle of the antenna.

—Flares of OH maser emission and significant changes in the structure of the spectra in 2023 and 2024, as well as a series of H₂O flares in 2023, may be associated with next accretion flare in S255 IR.

Of great interest is the monitoring of masers in the S255 IR to identify possible accretion flares, as well as high spatial resolution observations of OH to reveal the possible structure that OH maser condensations may form and, therefore, the structure of the magnetic field and its evolution.

ACKNOWLEDGMENTS

The authors express their gratitude to the staff of the Radio Astronomy Observatory in Pushchino and the Radio Astronomy Observatory in Nance (France) for their great assistance in conducting observations under the program of long-term monitoring of maser H₂O emission sources with the RT-22 radio telescope and maser OH emission sources with the Large Radio Telescope in Nance.

FUNDING

This work was supported by ongoing institutional funding. No additional grants to carry out or direct this particular research were obtained.

CONFLICT OF INTEREST

The authors of this work declare that they have no conflicts of interest.

REFERENCES

1. R. A. Burns, T. Handa, T. Nagayama, K. Sunada, and T. Omodaka, *Mon. Not. R. Astron. Soc.* **460**, 283 (2016).
2. T. R. Hunter, C. L. Brogan, G. MacLeod, C. J. Cyganowski, et al., *Astrophys. J. Lett.* **837**, L29 (2017).
3. M. P. Miralles, L. Salas, I. Cruz-González, and S. Kurtz, *Astrophys. J.* **488**, 749 (1997).
4. K. Y. Lo and B. F. Burke, *Astron. Astrophys.* **26**, 487 (1973).
5. B. E. Turner, *Astrophys. Lett.* **8**, 73 (1971).
6. N. J. Evans II, R. M. Crutcher, and W. J. Wilson, *Astrophys. J.* **206**, 440 (1976).
7. O. S. Bayandina, I. E. Val'tts, S. E. Kurtz, and N. N. Shakhvorostova, *Astrophys. J. Suppl.* **256**, 7 (2021).
8. A. Baudry, J. F. Desmurs, T. L. Wilson, and R. J. Cohen, *Astron. Astrophys.* **325**, 255 (1997).
9. A. D. Haschick, K. M. Menten, and W. A. Baan, *Astrophys. J.* **354**, 556 (1990).
10. K. M. Menten, *Astrophys. J. Lett.* **380**, L75 (1991).
11. R. P. Norris, J. B. Whiteoak, J. L. Caswell, M. H. Wieringa, and R. G. Gough, *Astrophys. J.* **412**, 222 (1993).
12. A. Caratti o Garatti, B. Stecklum, R. Garcia Lopez, J. Eisloffel, et al., *Nat. Phys.* **13**, 276 (2017).
13. L. Moscadelli, A. Sanna, C. Goddi, M. C. Walmsley, et al., *Astron. Astrophys.* **600**, L8 (2017).
14. T. Hirota, R. Cesaroni, L. Moscadelli, K. Sugiyama, R. A. Burns, J. Kim, K. Sunada, and Y. Yonekura, *Astron. Astrophys.* **647**, A23 (2021).
15. M. I. Pashchenko, E. E. Lekht, and I. I. Berulis, *Astron. Rep.* **45**, 600 (2001).
16. V. I. Slysh, M. I. Pashchenko, G. M. Rudnitskii, V. M. Vitrishchak, and P. Colom, *Astron. Rep.* **54**, 599 (2010).
17. N. T. Ashimbaeva, E. E. Lekht, M. I. Pashchenko, V. V. Krasnov, and A. M. Tolmachev, *Astron. Rep.* **66**, 648 (2022).
18. V. L. Fish and M. J. Reid, *Astrophys. J. Suppl.* **164**, 99 (2006).

Translated by E. Seifina

Publisher's Note. Pleiades Publishing remains neutral with regard to jurisdictional claims in published maps and institutional affiliations.